

Experimental study of a mechanism for absolute parametric instability in a nonuniform plasma

V. I. Arkhipenko, V. N. Budnikov, E. Z. Gusakov, A. N. Savel'ev, and L. V. Simonchik

A. F. Ioffe Physical Research Institute, Academy of Sciences of the USSR, Leningrad

(Submitted 19 January 1987)

Zh. Eksp. Teor. Fiz. **93**, 1221–1234 (October 1987)

The general properties of absolute parametric instabilities in a magnetoactive nonuniform plasma are studied experimentally for the particular case of the $l' \rightarrow l' + s$ decay process. Microwave diagnostics of the ion-acoustic noise which is excited have been employed and the role of feedback in the excitation process demonstrated. An instability mechanism is exhibited which is related to the nonuniformity of the plasma and the multimode nature of the pump wave.

1. INTRODUCTION

Parametric instabilities are the reason for anomalous absorption and reflection of electromagnetic radiation in experiments involving the use of lasers for inertial confinement fusion and the use of microwaves for plasma heating. Plasma density gradients have a strong stabilizing influence on such instabilities, not only raising their thresholds but also causing them to saturate at a relatively low level because the energy of the unstable waves convects out of the region of instability.¹ Under these conditions parametric processes are responsible for spatial convective amplification.

In previous work a number of different mechanisms have been analyzed that can be responsible for a real absolute parametric instability in such situations. In general it arises when even a fraction of the energy removed from the region of the three-wave resonance returns there, i.e., when a feedback loop is established.²⁻⁵ As a result of the resonant properties of this feedback, the spectrum of waves excited in the plasma may become narrow and change its shape, and the waves may become more unstable. An absolute instability saturates at a higher level due to nonlinear processes and in this sense is more dangerous.

It should be noted that as a rule these theoretical studies employ a slab model for the plasma and use the plane wave approximation for the pump wave, even though the experimental geometry is often quite complicated and the pump wave exhibits coherent spatial structure. It is well known that coherent spatial structures arising from the reflection of the pump and daughter waves play a major role in enhancing Raman scattering in uniform nonlinear optical media,⁶ and in exciting so-called double stimulated Brillouin scattering in the laser-produced plasma.⁷ We feel that in complicated plasma geometries other types of coherent spatial pump-wave structure associated, for example, with the directionality of the source of illumination or the way the wave propagates can give rise to feedback and consequently to absolute instability. In the present paper we investigate experimentally and theoretically a mechanism for the excitation of absolute parametric instability associated with the multimode character of the pump wave. We consider the case of an oblique electrostatic wave decaying into another oblique electrostatic wave and an ion acoustic wave in a magnetized plasma with density gradients normal and parallel to the magnetic field.

2. STATEMENT OF THE PROBLEM

The experiment was performed in the linear device Granit.⁸ A plasma with both longitudinal and transverse density gradients was produced by cyclotron breakdown in a chamber of diameter 2 cm and length 1 m (Fig. 1) located in an axial magnetic field $H = 3$ kG and filled with argon at a pressure of $1-2 \cdot 10^{-2}$ torr. The electron temperature was $T_e = 1-2$ eV and the density satisfied $n_e \lesssim 10^{12}$ cm⁻³. A waveguide 3 was used to excite an oblique electrostatic wave in the plasma at a frequency $\omega_0/2\pi = 2350$ MHz, principally in the fundamental radial Trivelpiece-Gould mode. The dispersion relation of the latter has the form $k_{\perp}^2 = [\omega_{pe}^2(r, z)/\omega^2 - 1]k_{\parallel}^2$, where k_{\parallel} and k_{\perp} are the components of the wave vector parallel and transverse to the magnetic field. This wave can propagate in a plasma whose density exceeds the critical value, $n > n_c$. For this mode the plasma near the axis acts as a waveguide with a weak longitudinal density gradient (6 in Fig. 1b). As the wave propagates in this waveguide in the direction of decreasing density, it slows down and its electric field increases in strength. Near the points at which the critical density surface intersects the chamber axis (focal points), where the oblique electrostatic wave is converted into a "warm-plasma wave," the electric field attains its maximum value:⁹

$$E_0 = \left(\frac{2P'_0}{\omega_0} \right)^{1/2} \frac{k_0^{3/2}}{(1+3r_a^2 b k_0^2)^{1/2}} \cdot \exp \left\{ i \int_{-\infty}^z (k_0 + i k_0'') dz' - \frac{k_0 r^2}{2b} - i \omega_0 t \right\} + \text{c.c.},$$

where $P'_0 = \kappa P_0$ is the portion of the power P_0 that goes into supplying the excitation of the fundamental, with $\kappa \approx 0.2$ (see Ref. 10); k_0 is the longitudinal wave number found by solving the equation

$$3r_a^2 k_n^2 - \frac{z}{a} - \frac{2(2n+1)}{k_n b} - i \varepsilon_{\parallel}'' = 0, \quad (1)$$

with $n = 0$; a and b are the density length scales for the plasma near the axis:

$$\varepsilon_{\parallel} = 1 - \frac{\omega_{pe}^2(r, z)}{\omega^2} + i \varepsilon_{\parallel}'' = \frac{z}{a} + \frac{r^2}{b^2} + i \varepsilon_{\parallel}'' ,$$

and k_0'' is the damping rate of the Trivelpiece-Gould mode due to electron-neutral collisions and Landau damping. The

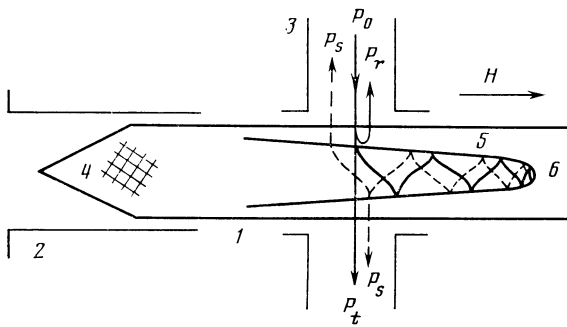


FIG. 1. Experimental layout: 1—discharge chamber; 2—3-cm band waveguide; 3—10-cm band waveguide; 4—region where plasma is formed by cyclotron breakdown; 5—critical surface; 6—focal point. P_0 , P_t , P_r , and P_s , respectively, are the input, transmitted, reflected, and scattered power.

collisional part of the damping has the form

$$\int_{-\infty}^z k_n'' dz' = (v/\omega) k_n a.$$

It is just in the neighborhood of the focal point, especially when the input power going into heating the plasma is quite low ($P_0 \leq 10$ mW), that one should expect nonlinear plasma effects to appear, e.g., the parametric instability $l_0 \rightarrow l'_0 + s$. This causes the reflected Trivelpiece-Gould mode and the ion-acoustic wave propagating in the direction of decreasing plasma density to grow. The instability threshold is defined not by the radial but by the axial plasma gradient.¹⁰ Since the decay condition

$$2k_0(z_0) = \omega_s/c_s \equiv k_s \quad (2)$$

(where ω_s and c_s are the frequency and velocity of the ion-acoustic wave) is satisfied for the $l_0 \rightarrow l'_0 + s$ process at only a single point, one should expect^{1,2} that the instability will

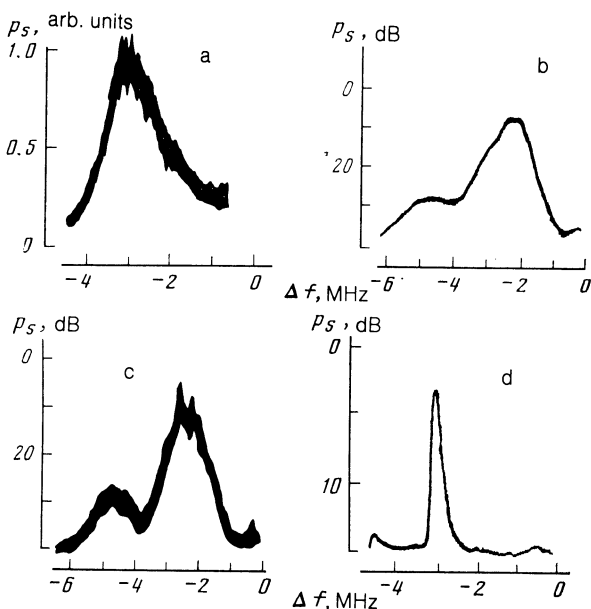


FIG. 2. Spectra of the scattered signal: (a)—in the convective amplification region; (b), (c), (d)—in the region of strong parametric reflection. The measurements (b) and (d) are continuous; (c) is pulsed.

give rise to spatial amplification of acoustic noise incident on the decay region. Thus the spectral density of the scattered wave is given by the expression¹⁰ $p_s = AS$, where the constant A is determined by the plasma noise level in the absence of the pump wave, and the amplification factor is

$$S = \exp 2\pi Z = \exp \frac{k_0 a E_0^2 (r=0)}{8n_e T_e}. \quad (3)$$

The first experiments¹¹ showed that when the power P_0 of the pump wave exceeds 20 mW, a satellite line appears in the spectrum of the signal reflected by the plasma in the waveguide transmission line, shifted in the red direction by $f_s = \omega_s/2\pi = 2-3$ MHz (Figs. 2a-c). Although the satellite frequency shift and the pump wave power threshold are satisfactorily explained by saying that this signal is generated at the focal point as a result of the $l_0 \rightarrow l'_0 + s$ decay, the dependence of satellite spectral density on the pump-wave power differs markedly from the form predicted theoretically [cf. Eq. (4), below]. This discrepancy has stimulated the experimental and theoretical studies described in detail in the present paper, preliminary results of which have already been communicated in a letter.¹²

3. AMPLITUDE OF THE SCATTERED WAVE AS A FUNCTION OF FREQUENCY

The spectral density of the parametrically reflected plasma wave p_s found experimentally as a function of the pump-wave power P_0 is shown in Fig. 3 for two parameter regimes. In the first regime (trace 1), the argon was at a pressure of $1.6 \cdot 10^{-2}$ torr and the electron energy distribution function (obtained using a multigrid analyzer) was Maxwellian with $T_e = 1$ eV; the density length scales were $a = 5$ cm and $b = 0.4$ cm. The second regime (trace 2) was obtained with an argon pressure of 10^{-2} torr. The electron distribution function had a pronounced tail of fast electrons with $T_h = 20$ eV, so that it was impossible to determine the temperature of the bulk of the electrons. Because the measurements in the second regime were not carried out in as much detail, only the results obtained in the first regime will be compared with the theoretical predictions.

As shown in Fig. 3, both $p_s(P_0)$ curves consist of two relatively slowly varying parts (I and III) on either side of a sharp rise (II). In region I p_s depends exponentially on P_0 , in

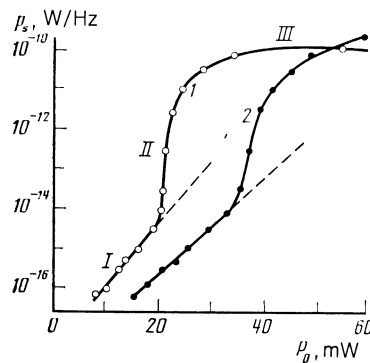


FIG. 3. Maximum value of the spectral density of the scattered signal as a function of pump-wave power for two regimes: I—convective amplification region; II—region of rapid growth; III—region of strong parametric reflection.

good agreement with the prediction (3) that scattering takes place off the equilibrium acoustic fluctuations.¹⁰ The amplification factor can be found from the experimental curves in Fig. 3 by means of the obvious expression

$$S(P_2) = (p_{s2}/p_{s1})^{P_2/(P_2-P_1)}, \quad (4)$$

where p_{s2} and p_{s1} are the amplitudes of the scattered signal corresponding to P_2 and P_1 . In the first regime the amplification factor ranged between 10 and $2 \cdot 10^3$ as the power was varied from 10 to 20 milliwatts; in the second it ranged between 10 and 10^4 as the power was varied from 15 to 25 milliwatts. The spectrum of the scattered signal in the first part of the range (Fig. 2a) was quite smooth, was shifted in the red direction by $f_0 - f = 3$ MHz, and had a width $\delta f = 0.9$ MHz. At higher values of the power and the spatial amplification factor (in the first regime, for $S > 2 \cdot 10^3$, and in the second, for $S > 10^4$), the satellite grew sharply. Its spectrum, measured using an S4-27 analyzer in the continuous mode, narrowed slightly to $\delta f \approx 0.5$ MHz. Sometimes it remained continuous but fluctuated strongly (Fig. 2b). At other times the plasma density near the entrance differed slightly and the spectrum exhibited jagged structure, with two to four sharp spikes (Fig. 2c).

When an S4-47 analyzer was used to sample the spectrum at $10\text{-}\mu\text{s}$ intervals, it revealed that the spectrum corresponding to Fig. 2b consists of a small number (from one to three) of narrow lines with $\delta f \lesssim 0.1$ MHz (Fig. 2d), separated by 0.3–0.5 MHz. The width and shape of the satellite and pump wave agree and are determined by how long the sampling window of the analyzer remained open. The frequency and amplitude of the lines changed from one measurement to the next. These variations are evidently related to fluctuations in the macroscopic plasma parameters resulting from discharge instability. Measurements made in the resonator showed that the plasma density varied by as much as 10%.

On the other hand, if the plasma density fluctuations were small, there was a small probability of detecting jagged peaked structure reproducing that observed in the continuous measurements (Fig. 2c). Thus the pulsed measurements showed that when the scattered wave was growing rapidly regardless of which regime the discharge was in, the spectrum narrowed markedly from $\delta f \approx 0.9$ MHz to $\delta f \lesssim 0.1$ MHz.

At the end of the sharply rising portion II of the $p_s(P_0)$ curve (see Fig. 3), both in the regular and the stochastic regimes, the level $p_s \approx 5 \cdot 10^{11}$ W/Hz implies that the pump wave underwent total parametric reflection in the neighborhood of the focus.¹⁰ As the power continued to increase in the range $40 \text{ mW} < P_0 < 100 \text{ mW}$, the satellite frequency shift decreased to $f_0 - f \lesssim 2$ MHz. The explanation for this is that total reflection of the wave took place in denser plasma and it was scattered off longer-wavelength oscillations.

4. SPATIAL STRUCTURE OF THE ION-ACOUSTIC FLUCTUATIONS

It is reasonable to suppose that the $p_s(P_0)$ profile steepens up and the scattered-wave spectrum becomes narrower because the system is approaching the threshold for the absolute parametric instability $l_0 \rightarrow l'_0 + s$. An experiment was performed to clarify the mechanism for this process by studying the spatial structure of the acoustic fluctuations.

This was done using an oblique electrostatic wave like the pump wave, but at a shifted frequency $f_\zeta = f_0 + \Delta f$. This wave was excited with the same waveguide used for the pump wave. The shifted wave scatters off parametrically excited acoustic waves at the point z_ζ defined by $2k_0(z_\zeta, f_\zeta) = k_s$, displaced from z_0 by a distance

$$\Delta z = z_\zeta - z_0 = -2\Delta f a / f_0. \quad (5)$$

Experimentally, the peak spectral density A_s of the satellite of the probe wave was measured as a function of the frequency shift $\Delta f = f_\zeta - f_0$ and converted into a function of position through expression (5).

The experimental procedure was as follows. In the absence of the pump wave ($P_0 = 0$), a probe wave power $P_{\zeta m}$ was fed into the plasma at the frequency f_ζ for which the satellite attained its maximum value $p_{s\zeta m}$. Then the power P_ζ was reduced by a factor of 100, causing the satellite to disappear (since this reduced the power substantially below the threshold level). Then the pump was turned on with power P_0 , the satellite of the probe wave $p_{s\zeta}$ appeared, and its amplitude (in dB relative to the maximum value $p_{s\zeta m}$) was read off. This technique is based on the principle that for an arbitrary frequency f_ζ the function $p_{s\zeta}(P_\zeta)$ accurately reproduces the shape of $p_s(P_0)$, although the absolute scales may be different. Since the shifts in the frequencies f_ζ and f_0 are relatively small, it is clear physically that the amplitudes of the maximum scattered signals at different frequencies in the plasma have to be the same, while the waves must arrive at the focus with identical amplitudes. The difference in the measured absolute values $p_{s\zeta m}$ and $P_{\zeta m}$ is evidently related to the frequency dependence of the coupling coefficient between the waveguide and the transmission line. The technique of measuring $p_{s\zeta}$ and P_ζ relative to the peak values $p_{s\zeta m}$ and the corresponding quantity $P_{\zeta m}$, described above, enabled us to eliminate this frequency dependence.

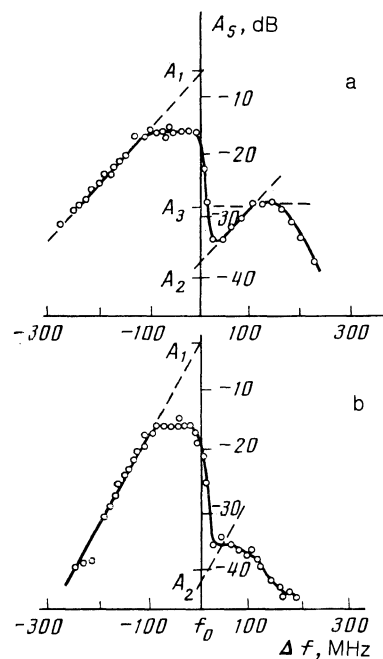


FIG. 4. Amplitude A_s of the satellite of the probe wave as a function of frequency separation: (a)—regime I; (b)—regime II.

Figure 4a, which displays the results of probe measurements in the first regime for $f_0 = 2335$ MHz, $P_0 = 50$ mW, $f_s = 2.1$ MHz, and $p_{s0} = p_{s0m}$, permits one to visualize how acoustic waves propagate and grow in the narrow (width 2–3 cm) region of parametric amplification localized near the linear conversion point.

Note that the present model of the $l_0 \rightarrow l'_0 + s$ parametric process would lead one to expect acoustic waves to occur in the region of the plasma with $n < n_c$ ($\Delta f < 0$), since ion sound must go directly there from where it originates, and to expect them to be absent for $n > n_c$ ($\Delta f > 0$). But the observations reveal a more complicated picture: noise is found in the region with $\Delta f > 0$ also, although with smaller amplitudes. We conjecture that the largest peak in $A_s(\Delta f)$ is associated with the region where spatial amplification takes place according to $l_0 \rightarrow l'_0 + s$, near the point $z = z_0$, where $2k_0(z_0) = k_s$. The exponentially decaying part of the function $A_s(\Delta f)$ seen for $\Delta f < -100$ MHz reflects damping of the ion-acoustic wave with distance from the instability region, given by $A_s \sim \exp(4k_s'' a \Delta f / f_0)$. The damping rate found from Fig. 4a, $k_s'' = 1.9 \text{ cm}^{-1}$, may be associated with both ion-neutral collisions and ion Landau damping, assuming $T_i/T_e \gtrsim 1/15$. The acoustic noise distribution (both shape and magnitude) is discussed in detail in Ref. 13. Here we only want to emphasize that the decrease in the acoustic noise level is already present for $\Delta f < 0$. This fact, as well as the steep slope for $0 < \Delta f < 35$ MHz, is easy to understand if we assume that the contribution to A_s comes not only from the amplified ion-acoustic wave, but also from stimulated modes arising as a result of low-frequency beating due to the pump-wave ponderomotive force and the scattered electrostatic wave. Calculations taking this into account agree well with the experimental data.

Passing to the interpretation of the A_s distribution for $\Delta f > 0$, we note that the noise in this region exceeds the thermal level by a factor of 10^6 – 10^7 . The noise is localized in the region $\Delta f < 200$ MHz; it disappears as we move in the direction of increasing plasma density. The shape of the noise distribution here, characterized by the presence of a maximum and by an exponential dropoff toward $\Delta f = 0$, makes it natural to suppose that the maximum is associated with the region where the noise is generated. The exponential decay suggests that it is damped while propagating toward the region where parametric amplification occurs. The question of the mechanism for sound generation will be investigated in detail below. For now we remark that if we take the two regions of exponential decay as spatial amplitude distributions of the noise coming from the region of parametric amplification ($\Delta f < 0$) and the incident noise ($\Delta f > 0$), respectively, then the difference between the quantities A_1 and A_2 intercepted on the ordinate evidently yields the amplification coefficient for an acoustic wave propagating in this region: $S = 10^{0.1(A_1 - A_2)} \approx 3 \cdot 10^3$. This is close to the value of S for which the function $p_s(P_0)$ departs from exponential in regime I (cf. Fig. 3). The results of probe measurements in regime II of Fig. 3 are shown in Fig. 4b. Here the pump power was $P_0 = 70$ mW, with $f_s = 2.6$ MHz. The amplification coefficient $S = 10^4$ obtained from Fig. 4b is close to the value associated with the sharp bend away from the exponential part of curve 2 of Fig. 3.

We proceeded somewhat differently in the probing experiment, where the frequency of the probing wave was held

fixed, while the pump-wave frequency varied. The results obtained were close to those represented in Fig. 4.

We next consider how sound is generated in the vicinity of the smaller maximum. The high level of acoustic noise may result from the interaction between the strong satellite of the l'_0 pump wave and a small admixture of the first radial Trivelpiece-Gould mode. The higher Trivelpiece-Gould modes must be excited close to the waveguide input, but their amplitude relative to that of the fundamental $n = 0$ mode decreases with n , mainly due to strong longitudinal retardation. The resonant point for the $l_1 \rightarrow l'_0 + s$ process is determined by the condition

$$k_0(z_1) + k_1(z_1) = \omega_s / c_s, \quad (6)$$

where $k_1(z)$ can be found from (2) with $n = 1$. The possibility of satisfying the resonant condition (6) is associated with the fact that the first mode is slowed down more than the fundamental, and the decrease in $k_0(z_1)$ relative to $k_0(z_0)$ is made up for by the inequality $k_1(z_1) > k_0(z_1)$. Using (2), (6), and the relation $2k_s(z_1, f_0 + \Delta f) = k_s$, it is not hard to show that for $f_s = 2.1$ MHz, $T_e = 2$ eV, and $b = 0.4$ cm, the probe wave with $\Delta f = 160$ MHz will scatter at the point z_1 , which is close to the x -coordinate of the smaller maximum in Fig. 4a. The theory predicts how the location of the maximum varies as a function of the frequency of the acoustic wave produced. We have verified this dependence experimentally. For this purpose the spatial structure of the acoustic waves was probed for various pump-wave power levels ($30 \text{ mW} < P_0 < 100 \text{ mW}$), corresponding to a range of ion-acoustic frequencies $3 \text{ MHz} > f_s > 32 \text{ MHz}$. The resulting dependence $\Delta f_{m1}(f_s)$ is shown in Fig. 5, where it is compared with the results calculated from Eqs. (2) and (6). Satisfactory qualitative and quantitative agreement is obtained. This may be regarded as confirming the proposed mechanism for sound generation through the $l_1 \rightarrow l'_0 + s$ process.

The fraction of energy carried by the first radial mode can be estimated from the following considerations. The power of the acoustic wave produced in the $l_1 \rightarrow l'_0 + s$ process for small amplitudes of the l_1 and l'_0 waves, as will be shown in the next section, can be written in the form

$$\bar{A}_s = 2\pi Z_{10} \frac{f_s}{f_0} P_{s0}(z_1), \quad (7)$$

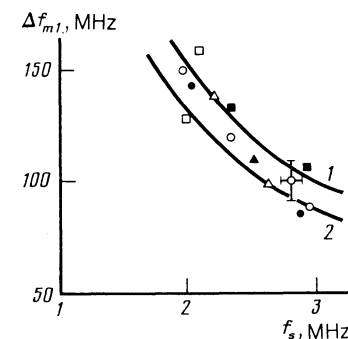


FIG. 5. Dependence of the frequency Δf_{m1} of the smaller maximum on the frequency of the excited ion-acoustic wave. Traces 1 and 2 are calculated for $T_e = 2$ and 1.5 eV, respectively.

where

$$\begin{aligned} Z_{10} = & \frac{P_1 a}{2\pi n_e T_e \omega_0} k_0^2 k_1^2 (k_0^2 + k_1^2) \exp \left[-2 \int_{-\infty}^{z_1} k_1'' dz' \right] \\ & \cdot \left\{ \left[3r_d^2 b k_0 k_1 (k_0 + k_1) + \frac{3k_0^2 + k_1^2}{k_1 k_0} \right] (k_0 + k_1)^2 \right\}^{-1}, \end{aligned}$$

which is analogous to (3), characterizes the strength of the parametric instability in the $l_1 \rightarrow l'_0 + s$ process; $k_0 = k(z_1)$; $k_1 = k_1(z_1)$; and $P_{s0}(z_1)$ is the power of the pump-wave satellite at the point z_1 .

The excitation of the acoustic wave and the amplification of the oblique electrostatic wave l'_0 are naturally accompanied by a decrease in the power of the pump wave l_1 , which may be estimated as follows. The number of phonons excited parametrically per unit time has to equal the number of incident pump-wave plasmons. But since a steady state is attained in the experiment, the decrease in the pump-wave plasmon flux must equal the flux of the resulting phonons. Thus the decrease in the pump-wave power can be written in the form

$$\begin{aligned} \Delta P_1 = & \frac{f_0}{f_s} \bar{A}_s = 2\pi Z_{10} P_{s0}(z_1) \left[P_1 \exp \left(-2 \int_{-\infty}^{z_1} k_1'' dz \right) \right]^{-1} \\ & \cdot P_1 \exp \left(-2 \int_{-\infty}^{z_1} k_1'' dz \right). \end{aligned}$$

For pump-wave powers $P_0 > 40$ mW, as stated above, the satellite is very strong, since it is associated with nearly complete parametric reflection. Calculation shows that for $P_0 = 50$ mW,

$$2\pi Z_{10} P_{s0}(z_1) \left[P_1 \exp \left(-2 \int_{-\infty}^{z_1} k_1'' dz \right) \right]^{-1} \approx 4,$$

i.e., for interaction with such a strong wave the l_1 wave must be totally depleted.

Since the two acoustic waves (the one incident on the spatial amplification region and the amplified wave at $P_0 = 50$ mW) are produced as a result of complete conversion of energy of the first and second Trivelpiece-Gould modes, respectively, into satellite energy, we can estimate the fraction of energy in the first radial mode from the ratio of the amplitudes of the two maxima in Fig. 4a. A more accurate calculation, taking into account the differences in radial structure in the incident and amplified acoustic waves, yields

$$\frac{P_1}{P'_0} = \exp \left[2 \int_{-\infty}^{z_1} k_1'' dz - 2 \int_{-\infty}^{z_0} k_0'' dz \right] \left[1 + \frac{1}{(k_s/k_1 - 1)^2} \right] 10^{A_1 - A_3}. \quad (8)$$

From Fig. 4a we find $P_1 = 0.08 P'_0$ in region I. In spite of its relatively small amplitude, the first mode gives rise to an important effect. Through the $l_1 \rightarrow l'_0 + s$ process it excites an ion-acoustic wave that carries part of the energy transported out of the $l_0 \rightarrow l'_0 + s$ decay region back into it. In other words, it introduces feedback. It is this feedback loop which is responsible for exciting the absolute instability, for producing the steepening in the $p_s(P_0)$ curve, and ultimately for the acoustic wave structure depicted in Fig. 4.

Note that such feedback cannot arise in a stratified slab medium, since the acoustic wave bringing the energy back would not be able to interact with the pump wave and with the same daughter wave because the transverse wave number resonance conditions can not be satisfied for both. In fact, in a stratified slab medium, the counterparts of the different radial modes of the pump wave are two plane waves l_0 and l_1 with different values of k_1 , i.e., $k_{10} \neq k_{11}$, which cannot both satisfy the conditions $k_{s1} = k_{10} - k_{11}$ and $k_{s1} = k_{11} - k'_1$. Thus an acoustic wave created in the $l_1 \rightarrow l'_0 + s$ process with a transverse wave number $k_{s1} = k_{11} - k'_1$ cannot take part in the $l_0 \rightarrow l'_0 + s$ process. It can interact with another daughter wave l'' , for which $k''_1 = k_{10} - k_{11} - k'_1$. In that case further amplification of acoustic noise can take place, but no feedback loop is established and consequently absolute instability is impossible.

On the contrary, in a two-dimensional plasma with density varying in both coordinate directions, where eigenmodes differ from plane waves, the $l_1 \rightarrow l'_0 + s$ process produces ion sound with a complicated transverse structure, with a very substantial component which is able to interact with l_0 and l'_0 waves. In our case the plasma has a large gradient in the transverse direction and the eigenmodes differ markedly from plane waves, and consequently the "feedback coefficient" is large. In our opinion, however, this effect is not intrinsic only to the present example, but has a wider significance. It will continue to play a role in plasma with a weak two-dimensional density variation, e.g., when the pump wave is a superposition of several plane waves propagating in a stratified slab plasma bounded in the transverse directions, or when the pump wave is a beam of finite width propagating parallel to the density gradient.

In the following section we will calculate the threshold and eigenfrequencies for the absolute instability. Here we describe the process of stimulating absolute instability, which also confirms the existence of the feedback loop. This effect is observed when a pump wave, with power close to the threshold for absolute instability, and a probe wave act on the plasma simultaneously. It is found that, even though the power is low and the frequency f_ξ differs from the pump-wave frequency substantially (by an amount many times greater than that of the excited ion-acoustic wave), the probe wave is able to increase the level of scattering of the pump wave severalfold.

The process of stimulation was studied quantitatively as follows. The pump-wave power was adjusted to the level $P_0 = 21$ mW, corresponding to the start of the steep region in the $p_s(P_0)$ dependence (Fig. 3). Then a probe wave was fed into the plasma at a frequency $f_\xi = f_0 + \Delta f$. By varying the probe wave power, we achieved a 5 dB increase in the pump-wave satellite. Figure 6 shows this power as a function of the minimum required frequency separation Δf . The vertical axis is also labeled with values of the amplification coefficient S corresponding to P_ξ , obtained using our Eq. (4) and the $p_{s\xi}(P_\xi)$ functional dependence. As Fig. 6 indicates, stimulation was obtained at comparatively low power only for probe wave frequencies satisfying $0 < \Delta f < 90$ MHz. The power required grows very sharply for $\Delta f > 90$ MHz, and for $\Delta f > 120$ MHz the scattered signal is damped rather than amplified, an effect related to the increase of Landau damping. In our opinion, it is comparatively easy to get amplifica-

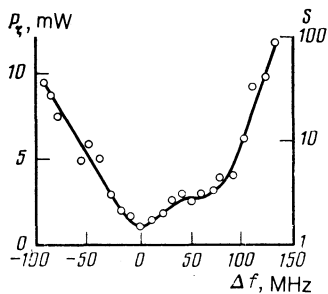


FIG. 6. Probe wave power required to stimulate absolute instability, plotted as a function of its frequency separation Δf .

tion of the scattered signal for $0 < \Delta f < 90$ MHz because in that case the probe wave interacts with sound through feedback between the points z_0 and z_1 . Thus the probe wave can coherently amplify acoustic noise circulating within the feedback loop and strongly influence the scattering level. When the point z_s leaves the loop ($z_s > z_1$), which happens, according to the calculation carried out for $f_s = 3$ MHz, at $\Delta f = 100$ MHz, this possibility goes away. For $\Delta f < 0$ stimulation is also possible in a system with two coupled pump-wave-probe-wave feedback loops, but it must take place at high probe wave power, as is observed experimentally. The power needed to observe stimulation also increases for $\Delta f < -90$ MHz.

5. DERIVATION OF THE DISPERSION RELATION

In order to develop a quantitative treatment of the $l \rightarrow l' + s$ absolute instability which occurs as a result of the mechanism described above, it is necessary to study the spatial amplification and propagation of an oblique electrostatic wave and its diffraction between the points z_1 and z_0 . We begin by considering the excitation of the Trivelpiece-Gould fundamental mode at the frequency $f_0 - f_s$ and the first radial harmonic of the Trivelpiece-Gould mode. Consistent with experiment, we assume that the amplitudes of the $n = 1$ mode are small and assume that the amplitudes of the high- n case the production of ion-acoustic waves is described by the equation

$$\Delta \frac{\delta n}{n} + k_s^2 \frac{\delta n}{n} = -\frac{1}{4\pi} \frac{\partial^2}{\partial z^2} \left(\frac{E_{0s} \cdot E_1}{nT_e} \right), \quad (9)$$

where the source term on the right hand side is the harmonic of the ponderomotive force with frequency f_s ,

$$E_1 = \left(\frac{2P_1}{\omega_0} \right) k_1^{1/2} \left(1 - \frac{k_1 r^2}{b} \right) (3 + 3r_d^2 b k_1^3)^{-1/2} \cdot \exp \left[\int_{-\infty}^z (ik_1 - k_1'') dz' - \frac{k_1 r^2}{2b} \right]$$

is the field of the first mode of the pump wave,

$$E_{0s} = \left(\frac{2}{\omega} \right)^{1/2} a_{out} k_0^{1/2} (1 + 3r_d^2 b k_0^3)^{-1/2} \cdot \exp \left[-\int_{z_c}^z (ik_0 - k_0'') dz' - \frac{k_0 r^2}{2b} \right]$$

is the field of the scattered wave with frequency $f_0 - f_s$, and

$$|a_{out}|^2 \exp \left[2 \int_{z_0}^z k_0'' dz' \right]$$

is the spectral density of the power transported by the satellite.

Equation (9) is easily solved for $\delta n/n$:

$$\frac{\delta n}{n} = \int \frac{\exp(ik_s R)}{R} \frac{1}{16\pi^2} \frac{\partial^2}{\partial z^2} \left(\frac{E_{0s} \cdot E_1}{nT_e} \right) d^3 r' \quad (10)$$

where

$$R = [(x-x')^2 + (y-y')^2 + (z-z')^2]^{1/2}.$$

In the region of interest to us, $z - z_1 \gg (x^2 + y^2)^{1/2}$, the integral over z' in (10) can be carried out using the method of stationary phase. The principal contribution to the integral comes from the three-wave resonance at $z = z_1$, defined by (6). If the fields E_{0s} and E_1 are localized in the region close to the axis, we can simplify the integrals with respect to x' and y' also, obtaining finally for the density of the irradiated sound wave the expression

$$\begin{aligned} \frac{\delta n}{n} = & -P_1^{1/2} a_{out}^* k_s (ab)^{1/2} (k_1 k_0)^{1/2} \\ & \cdot \left[1 - \frac{2k_1(z-z_1)}{k_s(z-z_1-ib)} + \frac{k_1 b r^2}{(z-z_1-ib)^2} \right] \\ & \cdot \{ 2\pi^{1/2} n_c T_e \omega_0 (z-z_1-ib) [k_1^2 (3r_d^2 b k_0^3 + 1) \\ & + k_0^2 (3r_d^2 b k_1^3 + 3)]^{1/2} \}^{-1} \\ & \cdot \exp \left\{ \int_{-\infty}^{z_1} (ik_1 - k_1'') dz' + \int_{z_0}^{z_1} (ik_0 + k_0'') dz' + ik_s(z-z_1) \right. \\ & \left. + \frac{ik_s r^2}{2(z-z_1-ib)} + i\frac{\pi}{4} \right\}. \quad (11) \end{aligned}$$

Using (11) we can easily calculate the power transported by the sound wave,

$$\bar{A}_s = \int_{-\infty}^{+\infty} \int dx dy 2c_s n_c T_e \left| \frac{\delta n}{n} \right|^2,$$

and show that it satisfies Eq. (7). This expression describes both the damping of a beam of sound waves, given by $k_s = \omega_s/c_s + ik_s''$, and diffraction, which is important for $z - z_1 > b$.

The limitations on the domain of validity of the procedure described above for deriving Eq. (11) arise because the $l_0 \rightarrow l'_1 + s$ process, in which the pump-wave fundamental mode excites an ion-acoustic wave and a scattered Trivelpiece-Gould mode at the first radial harmonic, occurs at the same time as the $l_1 \rightarrow l'_0 + s$ process at $z = z_1$. They can both be treated independently only if they both proceed sluggishly and if their respective coefficients of convective amplification are close to unity. In particular, for this to hold it is necessary that amplification be small in the $l_0 \rightarrow l'_1 + s$ process, i.e., $\ln S_{01} = 2\pi \tilde{Z}_{01} < 1$. If we take into account the calculations done by Arkhipenko *et al.*,¹⁰ this condition takes the form.

$$\begin{aligned} 2\pi \tilde{Z}_{01} = & \{ \kappa P_0 b k_0^3 k_1^3 (k_0^2 + k_1^2) (z-z_1) \\ & \cdot \exp \left(-\int_{-\infty}^{z_1} k_0'' dz \right) / 2\omega_0 T_e n_c (3r_d^2 b k_0^3 + 1) \\ & \cdot (3r_d^2 b k_1^3 + 3) k_s [k_s^2 - (k_0 + k_1)^2] \} < 1, \end{aligned}$$

where we have $k_0 = k_0(z_1)$, $k_1 = k_1(z_1)$, and $z \rightarrow z_1$. For the plasma parameters appropriate to the experiments, this criterion is not satisfied ($\pi \tilde{Z}_{01} \approx 2$), which raises the question of the applicability of Eq. (11).

For $2\pi \tilde{Z}_{01} > 1$ it is necessary to take into account simultaneously the $l_0 \rightarrow l'_1 + s$ and $l_1 \rightarrow l'_0 + s$ processes near $z = z_1$, and also to include the effect of the first radial mode of the pump wave on the propagation of scattered oblique electrostatic waves between $z = z_0$ and $z = z_1$. It is also necessary to treat the propagation and diffraction of the ion-acoustic wave between these points.

The problem is mathematically equivalent to that of solving a system of three coupled first-order differential equations for the amplitudes of the l'_0 and l'_1 modes and of sound in the neighborhood of the point $z = z_1$. Between the points z_0 and z_1 it is necessary to solve a system of coupled equations for l'_0 and l'_1 and an integrodifferential equation for the ion-acoustic wave. A rigorous treatment of this problem, the results of which will be published elsewhere, reveals that Eq. (11) correctly describes the amplitude of the sound wave generated at the point $z = z_1$ when $2\pi \tilde{Z}_{01} > 1$. The condition $\tilde{Z} > \tilde{Z}_{01}$ at the instability threshold is the actual criterion for the applicability of Eq. (11).

We turn now to the calculation of the spatial amplification of a sound wave described by Eq. (11) in the neighborhood of $z = z_0$. The efficiency with which sound waves are converted into scattered oblique electrostatic waves can be written¹⁰

$$\frac{a_{out}}{b_{in}} = T_{st} = (2\pi i)^{1/2} k_0^2 b P_0^{1/2} \cdot \exp \left[\int_{-\infty}^{z_0} (ik_0 - k_0'') dz + \frac{\pi \tilde{Z}}{2} \right] [2(3r_d^2 b k_0^3 + 1) \Gamma(i\tilde{Z} + 1)]^{-1}, \quad (12)$$

where $|a_{out}|^2$ is the power of the scattered oblique electrostatic wave near $z = z_0$, and

$$b_{in} = \int_0^{\infty} \frac{2k_0}{b} \exp\left(-\frac{k_0 r^2}{b}\right) \frac{\delta n}{n} \exp[-ik_s(z-z_0)] r dr. \quad (13)$$

Using Eqs. (11) and (13) to find the amplitude a_{out}^* corresponding to the incident sound wave and eliminate a_{out}^* from Eq. (12) and employing the asymptotic expression for the Γ -function in the case $\pi \tilde{Z} > 1$, we obtain the desired dispersion relation

$$1 + \left(\frac{2aP_1}{nT_e\omega_0} \right)^{1/2} (k_1 k_0)^{1/2} b \left[1 - \frac{2k_1}{k_s} \frac{z_0 - z_1 - ib}{z_0 - z_1 - 2ib} \right] \cdot \{ [k_1^2 (3r_d^2 b k_0^3 + 1) + k_0^2 (3r_d^2 b k_1^3 + 3)]^{1/2} (z_0 - z_1 - 2ib) \}^{-1} \cdot \exp \left\{ - \int_{-\infty}^{z_1} k_1'' dz + \int_{z_0}^{z_1} k_0'' dz - k_s'' (z_0 - z_1) + \pi \tilde{Z} \right\} \exp(i\Psi_0) = 0, \quad (14)$$

where

$$\Psi_0 = \frac{\omega_s}{c_s} (z_0 - z_1) + \int_{z_0}^{z_1} k_0(z) dz + \int_{-\infty}^{z_1} k_1(z) dz - \int_{-\infty}^{z_1} k_0(z) dz + \frac{\pi}{4} + \tilde{Z}(1 - \ln \tilde{Z}).$$

In a more rigorous treatment the dispersion relation retains

this form and differs from (14) only through the replacement of Ψ_0 by $\Psi_0 + \Delta\Psi$, where $|\Delta\Psi| \ll |\Psi_0|$. This dispersion relation imposes restrictions on the amplitude and phase of the feedback signal. As can be seen from (14), the amplitude condition can be written in the form $T_{st} b_l b_s T_{ls} = 1$ and implies a balance between the growth in the decay region, T_{st} , and losses through wave damping during propagation,

$$b_l = \exp \left[\int_{z_0}^{z_1} k_0'' dz \right], \quad b_s = \exp \left[- \int_{z_1}^{z_0} k_s'' dz \right],$$

and through scattering and diffraction of the ion-acoustic wave, T_{ls} . This condition allows the value of the spatial amplification coefficient to be determined at the threshold for absolute instability. If in (14) we substitute $k_1(z_1)$ and $k_0(z_0)$ calculated for $T_e = 2$ eV, $a = 5$ cm, $b = 0.4$ cm, and $f_s = 3$ MHz, use the results $P_1 = 0.08P_0$ and $k'' = 1.9$ cm⁻¹ found earlier for regime I, and take into account the Landau damping of the electrostatic waves, we obtain $S = \exp(2\pi \tilde{Z}) = 10^3$, close to the value observed experimentally.

The phase condition $\Psi = (2n + 1)\pi$ allows us to determine the frequencies of the acoustic waves excited in the absolute instability. Since the phase changes considerably in the feedback loop, we should anticipate that modes with large quantum numbers $n \gg 1$ will be excited. The frequency separation between modes n and $n + 1$ is given by

$$\delta f = \left(\frac{\partial \Psi}{\partial f_s} \right)^{-1} \approx \frac{c_s}{z_0 - z_1}. \quad (15)$$

This expression yields the estimates $\delta f \approx 0.5$ MHz for $f_s = 3$ MHz and $\delta f \approx 0.25$ MHz for $f_s = 2$ MHz. Note that in the regular scattering regime we observed multicomponent spectra (see Fig. 2c) with frequencies $f_s = 3.5, 3,$ and 2.6 MHz. As the frequency difference $f_0 - f$ decreased, the distinct peaks in the scattered signal approached one another and the quantity δf reached 0.3 MHz.

Equation (14) also enables us to find the growth rate of the $l \rightarrow l' + s$ absolute instability. Above threshold it is given by

$$\gamma = \pi \tilde{Z} c_s / (z_0 - z_1), \quad (16)$$

which provides an explanation for the fast ($\sim 1-2 \mu s$) times for establishing the scattered signal.¹²

6. CONCLUSION

In this work a new mechanism for exciting an absolute parametric instability in nonuniform plasmas has been predicted theoretically and studied experimentally. This mechanism arises in plasmas with density profiles which are functions of two or more spatial coordinates. It is associated with the presence of well developed coherent spatial structure in the pump wave. Theoretical ideas about the role played by the "feedback loop" in the process of exciting absolute parametric instability in nonuniform plasmas have for the first time received experimental confirmation. The existence of a regular regime of parametric reflection has been shown experimentally.

We would like to close by thanking A. D. Piliya, V. P. Silin, V. T. Tikhonchuk, and V. I. Fedorov for their interest in this work and for fruitful discussions of the results.

- ¹A. D. Piliya, Proc. 10th Conf. on Phenomena in Ionized Gases, Oxford (1971), p. 320.
- ²M. N. Rosenbluth, Phys. Rev. Lett. **29**, 565 (1972).
- ³A. D. Piliya, Pis'ma Zh. Eksp. Teor. Phys. **17**, 374 (1973) [JETP Lett. **17**, 266 (1973)].
- ⁴D. Pesme, G. Laval, and R. Pellat, Phys. Rev. Lett. **31**, 203 (1973).
- ⁵E. Z. Gusakov and A. D. Piliya, Fiz. Plazmy **6**, 509 (1980) [Sov. J. Plasma Phys. **6**, 277 (1980)].
- ⁶M. M. Sushinskii, *Sovremennye Problemy Spektroskopii Kombinatsionnogo Rasseyaniya (Current Problems of Raman Scattering Spectroscopy)*, Nauka, Moscow (1978), p. 187.
- ⁷A. A. Zozulya, V. P. Silin, and V. T. Tikhonchuk, Pis'ma Zh. Eksp. Teor. Fiz. **38**, 48 (1983) [JETP Lett. **38**, 52 (1983)].
- ⁸V. I. Arkhipenko, V. N. Budnikov, I. A. Romanchuk, and A. D. Piliya, Fiz. Plazmy **7**, 396 (1981) [Sov. J. Plasma Phys. **7**, 216 (1981)].
- ⁹V. N. Budnikov, V. I. Varfolomeev, K. M. Novik, and A. D. Piliya, Fiz. Plazmy **6**, 1050 (1980) [Sov. J. Plasma Phys. **6**, 576 (1980)].
- ¹⁰V. I. Arkhipenko, V. N. Budnikov, E. Z. Gusakov, *et al.*, Zh. Tekh. Fiz. **55**, 298 (1985) [Sov. Phys.—Tech. Phys. **30**, 174 (1985)].
- ¹¹V. I. Arkhipenko, V. N. Budnikov, E. Z. Gusakov, *et al.*, Abstract, Proc. 3rd Inter. Conf. on Interaction of Electromagnetic Radiation with Plasma, Alma-Ata (1982), p. 51.
- ¹²V. I. Arkhipenko, V. N. Budnikov, E. Z. Gusakov, *et al.*, Pis'ma Zh. Eksp. Teor. Fiz. **39**, 453 (1984) [JETP Lett. **39**, 549 (1984)].
- ¹³V. I. Arkhipenko, V. N. Budnikov, E. Z. Gusakov, *et al.*, Fiz. Plazmy **13**, 693 (1987) [Sov. J. Plasma Phys. **13**, 398 (1987)].

Translated by David L. Book